Physics of the atmospheric escape driven by EUV photoionization heating: Classification of the hydrodynamic escape in close-in planets

Hiroto Mitani[1] , Riouhei Nakatani[2] and Naoki Yoshida[1,3,4]

[1]Department of Physics, School of Science, The University of Tokyo, 7-3-1 Hongo, Bunkyo, Tokyo 113-0033
email: hiroto.mitani@phys.s.u-tokyo.ac.jp

[2]RIKEN Cluster for Pioneering Research, 2-1 Hirosawa, Wako, Saitama 351-0198, Japan

[3]Kavli Institute for the Physics and Mathematics of the Universe (WPI), UT Institutes for Advanced Study, The University of Tokyo, Kashiwa, Chiba 277-8583, Japan

[4]Research Center for the Early Universe, School of Science, The University of Tokyo, 7-3-1 Hongo, Bunkyo, Tokyo 113-0033

Abstract. The intense extreme ultraviolet radiation heats the upper atmosphere of close-in exoplanets and drives the atmospheric escape. The escaping process determines the planetary evolution of close-in planets. The mass loss rate depends on the UV flux at the planet. We introduce the relevant physical quantities which describe the dominant physics in the atmosphere. We find that the equilibrium temperature and the characteristic temperature determine whether the system becomes energy-limited or recombination-limited. We classify the observed close-in planets using the physical conditions. We also find that many of the Lyman-α absorptions detected planets receive intenser flux than the critical flux which can be determined from physical conditions. Our classification method can quantitatively reveal whether the EUV is not strong enough to drive the outflow or the Lyman-α absorption is not detected for some reason (e.g. stellar wind confinement). We also discuss the thermo-chemical structure of hydrodynamic simulations with the relevant physics.

Keywords. hydrodynamics – methods: numerical – planets and satellites: atmospheres – planets and satellites: physical evolution

1. Introduction

The close-in exoplanets lose their atmosphere due to the intense radiation from the host star. Understanding the mass loss process is necessary for the evolution of close-in planets. The process can be an origin of the statistical properties of observed exoplanets like sub-Neptune desert (Fulton et al. 2017; Owen & Wu 2017). In a typical hot Jupiter, extreme ultraviolet (EUV; > 13.6 eV) photons photoionize the hydrogen atoms and the photoelectrons thermalize into gas. The EUV heating process drives the atmospheric escape. There are some theoretical models of the atmospheric escape (Murray-Clay et al. 2009; Tripathi et al. 2015). Radiation hydrodynamics simulations have revealed the thermo-chemical structure of the upper atmosphere and the importance of such escaping processes in planetary evolution.

Previous theoretical studies calculate the mass loss rate due to the EUV heating. Some planetary evolution models have assumed the mass loss rate is proportional to the EUV flux but radiation hydrodynamic simulations have revealed the assumption is not correct every time. In the high UV case, the system becomes recombination-limited. In the recombination-limited regime, the photoionization rate and the recombination rate are balanced and the UV energy is lost to the radiative recombination energy. The mass loss rate is not proportional to the UV flux and is proportional to the square root of the UV flux.

Transit observations have revealed the existence of such escaping outflow (Vidal-Madjar et al. 2003; Ehrenreich et al. 2015). Recent observations have found that the close-in planets without Lyman-α absorption despite the intense UV irradiation (Rockcliffe et al. 2021). The physical conditions which determine the thermo-chemical structure are still unknown though it is important to understand the observed signatures.

Understanding physics in the upper atmosphere is necessary for the planetary evolution theory. We perform the radiation hydrodynamic simulations and construct a theoretical model to understand the escaping outflow in the observed exoplanets using the relevant physical quantities.

2. Relevant physical quantities

The important physical processes in the atmospheric escape are the photoheating, the planetary gravity, and the gas expansion. We can define the relevant temperatures and timescales in the upper atmosphere with photoionization heating. The characteristic temperature is given as (Begelman et al. 1983):

$$kT_{\mathrm{ch}} = \frac{\Gamma}{c_p/\mu m_{\mathrm{H}}} \frac{R_p}{c_{\mathrm{ch}}} \tag{2.1}$$

where Γ is the photoheating rate, R_p is the planetary radius, c_p is the specific heat at constant pressure, μ is the mean molecular weight, and m_H is the mass of the hydrogen atom. The right-hand side represents the deposited EUV energy in the characteristic sound crossing time. The characteristic sound speed c_{ch} is given as:

$$c_{\mathrm{ch}} = \left(\frac{\Gamma R_p}{c_p}\right)^{1/3} \tag{2.2}$$

The typical value of the sound speed in the upper atmosphere is $\sim 10\,\mathrm{km/s}$. The characteristic temperature represents how rapid the photoheating is compared to the gas expansion and does not mean the typical temperature of the system. In the case of EUV photoionization heating of hydrogen atoms, the photoheating rate is given as:

$$\begin{aligned}
\Gamma &= \frac{1-x}{m} F_0 \delta \langle \sigma \rangle \langle \Delta E \rangle \tag{2.3} \\
&= 1.2 \times 10^7 \,\mathrm{erg\,g^{-1}\,s^{-1}} \left(\frac{1-x}{0.5}\right) \left(\frac{m}{1.4 m_{\mathrm{H}}}\right) \left(\frac{\Phi}{10^{41}\,\mathrm{s^{-1}}}\right) \tag{2.4} \\
&\quad \times \left(\frac{r}{1\mathrm{au}}\right)^{-2} \left(\frac{\delta \langle \sigma \rangle \langle \Delta E \rangle}{10^{-18}\,\mathrm{cm^2} \times 1\,\mathrm{eV}}\right) \tag{2.5}
\end{aligned}$$

where x is the ionization degree, m is the gas mass per hydrogen nucleus, Φ is the EUV photon flux, δ is the attenuation factor, $\langle \sigma \rangle$ is the average cross-section of the photoionization and $\langle \Delta E \rangle$ is the average deposited energy per photoionization. The rate depends on the spectral shape. At higher energies, the cross section is smaller but the deposited energy increases, so these effects cancel each other out overall.

The equilibrium temperature T_{eq} can be determined from the balance of the photoheating and the cooling and becomes $\sim 10^4$ K for EUV photoionization heating of hydrogen atoms.

The gravitational temperature is given as:

$$T_g = \frac{GM_p \mu m_H}{R_p k} \tag{2.6}$$

The temperature indicates the strength of the planetary gravity. We can also define the gravitational radius $R_g = GM_p/c_{eq}^2$ using the sound speed at the equilibrium temperature c_{eq}.

The ratio between T_{ch} and T_{eq} is

$$\frac{T_{ch}}{T_{eq}} = \left(\frac{R_p \Gamma}{c_{eq}^3 c_p} \right)^{2/3} = \left(\frac{R_p}{R_g} \right)^{2/3} \left(\frac{\Gamma G M_p}{c_p c_{eq}} \right)^{2/3} \tag{2.7}$$

From the second factor, we can define the critical flux as:

$$F_{cr} = \frac{m c_p c_{eq}^5}{G M_p \sigma \Delta E} \tag{2.8}$$

$$= 5.8 \times 10^{12} \, \text{cm}^{-2} \, \text{s}^{-1} \left(\frac{m}{1.4 m_H} \right) \left(\frac{c_{eq}}{10 \, \text{km s}^{-1}} \right)^5 \tag{2.9}$$

$$\times \left(\frac{M_p}{M_J} \right)^{-1} \left(\frac{\sigma_0}{5 \times 10^{-18} \, \text{cm}^2} \right)^{-1} \left(\frac{\Delta E}{1 \, \text{eV}} \right)^{-1} \left(\frac{c_p}{5/2} \right) \tag{2.10}$$

and the ratio can be given as:

$$\frac{T_{ch}}{T_{eq}} \sim \xi^{2/3} \left(\frac{F_0}{F_{cr}} \right)^{2/3} \tag{2.11}$$

where $\xi = R_p/R_g$.

We can also define the photoheating timescale and the gravitational timescale:

$$t_g = \sqrt{\frac{R_p^3}{GM_p}} \tag{2.12}$$

$$t_h = \frac{R_p}{c_{ch}} \tag{2.13}$$

The ratio between the gravitational and photoheating timescales is

$$\frac{t_g}{t_h} = \xi^{5/6} \left(\frac{F_0}{F_{cr}} \epsilon (1-x) \right)^{1/3} \tag{2.14}$$

which represents the relative strength of the gravity to that of the photoheating. ϵ is an attenuation factor that depends on the column density of the hydrogen. If the ratio is larger than unity $t_g/t_h > 1$, the photoheating is faster and the system loses the atmosphere quickly.

We run radiation hydrodynamics simulations with the EUV photoionization and the recombination of hydrogen atoms to understand thermo-chemical structure of the atmosphere. In the simulations, we assume the Ly-α cooling is the dominant radiative cooling process as in the previous studies. We run simulations for the high EUV case ($T_{ch} > T_{eq}$) and the low EUV case ($T_{ch} < T_{eq}$) for typical hot Jupiter ($M_p = 0.7 M_J$, $R_p = 1.4 R_J$). Figure 1 shows the radial profile of the heating and cooling in our simulations. We find that the adiabatic cooling dominates in the case of low EUV and the Ly-α cooling dominates in the case of high EUV planets. T_{ch}/T_{eq} can be used to distinguish the dominant
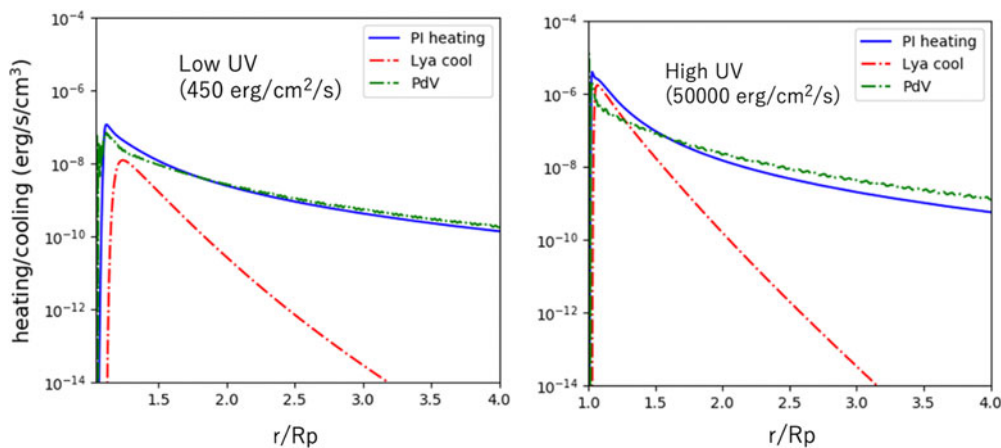
Figure 1. The radial profile of the heating and cooling rate. The ratio between the characteristic temperature and the equilibrium temperature is less than unity ($T_{\mathrm{ch}} < T_{\mathrm{eq}}$) in the low UV case (left) and larger than unity ($T_{\mathrm{ch}} > T_{\mathrm{eq}}$) in the high EUV case (right).

cooling process and whether the system is energy-limited or recombination-limited. In the typical hot Jupiters, $T_{\mathrm{eq}} = T_{\mathrm{ch}}$ when the UV flux is $\sim 10^3$ erg/cm^2/s and this value is consistent with the previous simulations.

3. Classification of the planetary atmosphere

The two physical conditions $t_g = t_h$ and $T_{\mathrm{ch}} = T_{\mathrm{eq}}$ can be drawn by a straight line on the $\log(F_0/F_{\mathrm{cr}}) - \log \xi$ plane. We investigate the conditions in the observed exoplanets using the open dataset (Schneider et al. 2011). We choose close-in planets with the orbital period $P < 10$ day. The EUV flux is intense in the case of a young host star. We estimate the EUV luminosity using the empirical relationships in (Sanz-Forcada et al. 2011)

$$\log L_{\mathrm{EUV}} = 29.12 - 1.24 \log \tau \tag{3.1}$$

where τ is the stellar age in Gyr. For stars whose ages were not listed in the catalog, we assumed the solar EUV luminosity. Figure 2. shows the distribution of the observed exoplanets in $\log(F_0/F_{\mathrm{cr}}) - \log \xi$ plane. The two conditions above can be drawn by two straight lines in the plane. The atmospheric escape in observed planets can be classified by two lines. We find that the EUV flux is lower than the critical flux in the case of the two of the Ly-α non-detected planets and the mass-loss is weak. K2-25 b receives intense EUV radiation from the host star and the EUV flux is larger than the critical flux. The planet does not show the Ly-α absorption (Lecavelier des Etangs et al. 2012; Rockcliffe et al. 2021). It may mean that unknown factors (e.g. stellar wind confinement (Carolan et al. 2020; Mitani et al. 2022), intense photoionization of the outflow) reduce the absorption signal. The $T_{\mathrm{eq}} = T_{\mathrm{ch}}$ condition can be used to quantitatively distinguish whether the EUV is not strong enough to drive the outflow. Future hydrodynamic simulations incorporating the effects of stellar winds, flares, and CMEs, and transit observations other than Ly-α are important to understand the structure of the outflow of these planets. There is few planets above $t_g = t_h$ line. The strong mass-loss reduces the planetary radius and planets above the line may move to the left side. In this plane, the young planets are in the upper part. If we assume the planetary radius weakly depends on the mass, ξ becomes smaller as the planet evolves and the old planets move to the left bottom part of the plane.
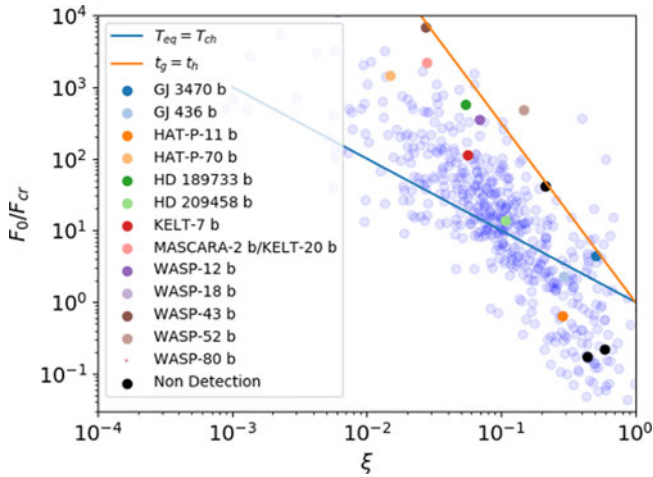
Figure 2. Observed close-in planets in $\log(F_0/F_{cr}) - \log \xi$ plane. Colored points represent H detected planets and the black dots represent the planets with Ly-α non-detection. Blue points represent other discovered close-in planets. Two straight lines show the physical conditions which we derived (Blue; $T_{eq} = T_{ch}$, Orange $t_g = t_h$).

We only consider the planetary gravity but the stellar gravity also plays an important role in gas kinematics around the hill radius. It is known that stellar gravity boosts the mass-loss rate, and there are formulas for planetary atmospheric dissipation rates that take this effect into account (Erkaev et al. 2007).

We also consider the timescale around the hill radius.

$$t_{h\_hill} = \frac{R_{hill}}{(\Gamma R_{hill}/c_p)^{1/3}} \tag{3.2}$$

$$t_{g\_hill} = \sqrt{\frac{a^3}{GM_*}} \tag{3.3}$$

where $R_{hill} = a\sqrt{M_p/3M_*}$ is the hill radius.

We find that the timescales can be used to determine whether the stellar gravity enhances the mass loss rate. When t_{h_hill}/t_{g_hill} is less than unity, the effect of the stellar gravity is small and photoheating energy dominates the system energy. On the bottom part of $\log(F_0/F_{cr}) - \log \xi$ plane, the ratio is less than unity. We find that the host star's gravity boosts the escape when the semi-major axis is less than 0.1 AU.

4. Discussion

FOSSATI: How do you define the equilibrium temperature?

MITANI: We can define the equilibrium temperature from photoheating and recombination cooling balance. The temperature is about 10^4 K in the case of EUV photoionization heating. This definition is different from the normal equilibrium temperature determined from the balance of radiation between the host star and the planet, which is usually used.

VIDOTTO: How do you treat the excess energy goes into heating in your characteristic temperature? In some models, the heating efficiency is used.

MITANI: The photoionization heating rate depends on the UV spectrum. We use the average deposited energy and cross-section to define the characteristic temperature. We do not use the heating efficiency as a parameter.

References

Begelman, M. C., McKee, C. F., & Shields, G. A. 1983, ApJ, 271, 70. doi:10.1086/161178

Carolan, S., Vidotto, A. A., Plavchan, P., et al. 2020, MNRAS, 498, L53

Ehrenreich, D., Bourrier, V., Wheatley, P. J., et al. 2015, Nature, 522, 459

Erkaev, N. V., Kulikov, Y. N., Lammer, H., et al. 2007, A&A, 472, 329

Fulton, B. J., Petigura, E. A., Howard, A. W., et al. 2017, AJ, 154, 109

Lecavelier des Etangs, A., Bourrier, V., Wheatley, P. J., et al. 2012, A&A, 543, L4

Mitani, H., Nakatani, R., and Yoshida, N. 2022, MNRAS, 512, 855

Murray-Clay, R. A., Chiang, E. I., & Murray, N. 2009, ApJ, 693, 23

Owen, J. E. & Wu, Y. 2017, ApJ, 847, 29

Rockcliffe, K. E., Newton, E. R., Youngblood, A., et al. 2021, AJ, 162, 116

Sanz-Forcada, J., Micela, G., Ribas, I., et al. 2011, A&A, 532, A6

Schneider, J., Dedieu, C., Le Sidaner, P., et al. 2011, A&A, 532, A79

Tripathi, A., Kratter, K. M., Murray-Clay, R. A., et al. 2015, ApJ, 808, 173

Vidal-Madjar, A., Lecavelier des Etangs, A., Désert, J.-M., et al. 2003, Nature, 422, 143